Molecular Biology of the Cell
Vol. 20, 5026–5035, December 1, 2009

A Mutation Associated with CMT2A Neuropathy Causes Defects in Fzo1 GTP Hydrolysis, Ubiquitylation, and Protein Turnover

Elizabeth A. Amiott,* Mickael M. Cohen,† Yann Saint-Georges,‡ Allan M. Weissman,† and Janet M. Shaw*

*Department of Biochemistry, University of Utah School of Medicine, Salt Lake City, UT 84112; †Laboratory of Protein Dynamics and Signaling, National Cancer Institute, Frederick, MD 21702; and ‡Institut de Génétique et Microbiologie, Université Paris-sud, 91405 Orsay Cedex, France

Submitted July 27, 2009; Revised September 24, 2009; Accepted September 28, 2009
Monitoring Editor: Thomas D. Fox

Charcot-Marie-Tooth disease type 2A (CMT2A) is caused by mutations in the gene *MFN2* and is one of the most common inherited peripheral neuropathies. Mfn2 is one of two mammalian mitofusin GTPases that promote mitochondrial fusion and maintain organelle integrity. It is not known how mitofusin mutations cause axonal degeneration and CMT2A disease. We used the conserved yeast mitofusin *FZO1* to study the molecular consequences of CMT2A mutations on Fzo1 function in vivo and in vitro. One mutation (analogous to the CMT2A I213T substitution in the GTPase domain of Mfn2) not only abolishes GTP hydrolysis and mitochondrial membrane fusion but also reduces Mdm30-mediated ubiquitylation and degradation of the mutant protein. Importantly, complexes of wild type and the mutant Fzo1 protein are GTPase active and restore ubiquitylation and degradation of the latter. These studies identify diverse and unexpected effects of CMT2A mutations, including a possible role for mitofusin ubiquitylation and degradation in CMT2A pathogenesis, and provide evidence for a novel link between Fzo1 GTP hydrolysis, ubiquitylation, and mitochondrial fusion.

INTRODUCTION

Mitochondrial dynamics, and fusion in particular, are essential for mammalian development and neuronal function (Chen *et al*., 2003; Hollenbeck, 2005; Chen and Chan, 2006; Detmer and Chan, 2007b). Mitochondrial fusion maintains mitochondrial networks and promotes the regular intermixing of lipids and matrix contents to preserve organelle function (Nunnari *et al*., 1997; Nakada *et al*., 2001; Ono *et al*., 2001; Chen *et al*., 2005; Detmer and Chan, 2007b). An important mitochondrial fusion GTPase, *fuzzy onions* or Fzo, was first identified in *Drosophila melanogaster* (Hales and Fuller, 1997). Subsequent studies of the budding yeast homologue *FZO1* have greatly expanded our understanding of the role this protein plays in mitochondrial outer membrane fusion (Hermann *et al*., 1998; Rapaport *et al*., 1998; Meeusen *et al*., 2004; Okamoto and Shaw, 2005; Meeusen and Nunnari, 2007). Fzo1 is an integral outer mitochondrial membrane protein containing a GTPase domain, three heptad repeat (HR) or putative coiled-coil domains, and a bipartite transmembrane region (Figure 1). Fzo1 is required for the maintenance of tubular mitochondrial networks, mitochondrial DNA (mtDNA) stability, and respiratory activity in yeast (Hermann *et al*., 1998; Rapaport *et al*., 1998; Sesaki and Jensen, 1999). Two *FZO1* homologues, termed mitofusins, are expressed in mammals (*MFN1* and *MFN2*) (Santel and Fuller, 2001; Rojo *et al*., 2002; Chen *et al*., 2003; Eura *et al*., 2003). Mitofusin proteins are thought to self-interact via their C-terminal coiled-coil domains, forming homo- and heterotypic oligomeric complexes. These interactions are proposed to "tether" adjacent mitochondria as an early step in the fusion process (Koshiba *et al*., 2004). The GTPase activity of Fzo1 and mitofusins is also essential for membrane fusion, but the actual step(s) in the fusion reaction that requires GTP hydrolysis is still debated (Hermann *et al*., 1998; Ishihara *et al*., 2004; Koshiba *et al*., 2004; Griffin and Chan, 2006).

Charcot-Marie-Tooth disease type 2A (CMT2A) is a peripheral neuropathy caused by autosomal dominant inheritance of mutations in the human mitofusin gene *MFN2* (Zuchner *et al*., 2004; Kijima *et al*., 2005; Lawson *et al*., 2005; Verhoeven *et al*., 2006). In CMT2A patients, axonal degeneration of the peripheral nerves that innervate the feet, lower limbs, and hands causes progressive sensory loss, weakness, and distal muscle atrophy. Some patients also develop optic atrophy and CNS abnormalities (Skre, 1974; Zuchner *et al*., 2004, 2006; Lawson *et al*., 2005; Chung *et al*., 2006). Approximately 60 CMT2A alleles have been identified throughout the *MFN2* gene. Most encode proteins with point mutations in and around the Mfn2 GTPase domain. Interestingly, there is no clear correlation between disease severity and the location of the mutation within the gene. Current models propose that mutant Mfn2 proteins preferentially affect neurons because these cells rely heavily on the proper delivery

This article was published online ahead of print in *MBC in Press* (http://www.molbiolcell.org/cgi/doi/10.1091/mbc.E09–07–0622) on October 7, 2009.

Address correspondence to: Janet M. Shaw (shaw@biochem.utah.edu).

Abbreviations used: CMT2A, Charcot-Marie Tooth Disease type 2A; coIP, coimmunoprecipitation; *FZO1*, yeast *fuzzy onions* gene; GDP, guanosine diphosphate; GTP, guanosine triphosphate; HA, hemagglutinin; HR, heptad repeat; IP, immunoprecipitation; MEF, mouse embryonic fibroblast; *MFN1*, mitofusin 1 gene; *MFN2*, mitofusin 2 gene; mito-GFP, mitochondrial matrix-targeted green fluorescent protein; mito-RFP, mitochondrial matrix-targeted red fluorescent protein; TEM, transmission electron microscopy.

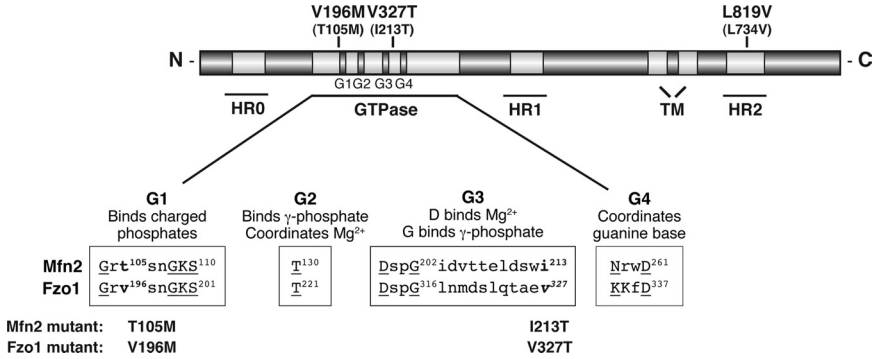

Figure 1. Schematic representation of Fzo1 domain structure, including three heptad repeat regions (HR0–HR2), a GTPase domain (including conserved GTPase motifs G1–G4) and a transmembrane region (TM). Fzo1 amino acid substitutions analogous to human Mfn2 mutations found in CMT2A patients (in parentheses) are indicated. Below, the GTPase domain is expanded to show the alignment of Mfn2 and Fzo1 protein sequences in the conserved G1–G4 motifs.

of functional mitochondria to synapses and other regions that require a high concentration of mitochondria for calcium buffering and ATP production (Verstreken *et al*., 2005; Chen and Chan, 2006; Baloh, 2008; Cartoni and Martinou, 2009).

Although mitofusins are highly conserved and essential for mitochondrial fusion, several reports suggest that Mfn1 and Mfn2 may perform nonoverlapping functions in addition to their roles as fusion molecules. Examples of the reported differences in Mfn1 and Mfn2 activity include 1) a notable difference in the shape and motility of mitochondrial fragments in Mfn1 and Mfn2 knockout mouse embryonic fibroblasts (MEFs) (Chen *et al*., 2003); 2) dissimilar GTP hydrolysis activities for Mfn1 and Mfn2 (Ishihara *et al*., 2004); 3) functional cooperation between the inner membrane fusion protein Opa1 and Mfn1 but not Mfn2 (Cipolat *et al*., 2004); 4) distinct interactions of Mfn1 and Mfn2 with the Bcl-2 family members Bak and Bax (Karbowski *et al*., 2002; Brooks *et al*., 2007); 5) implication of Mfn2 as a player in multiple signaling pathways (McBride *et al*., 2006; de Brito and Scorrano, 2008b); and 6) a role for Mfn2 (but not Mfn1) in maintaining mitochondria-ER contacts (de Brito and Scorrano, 2008a, 2009). The fact that no *MFN1* mutations have been identified in CMT2A patients further suggests that CMT2A disease may result from disruption of an activity that is unique to Mfn2.

The effect of CMT2A alleles on mitochondrial shape, fusion, function, and motility has been examined in various cell types and model systems. Analysis of CMT2A patient fibroblasts harboring various *MFN2* mutations revealed normal mitochondrial morphology and distribution, mitochondrial fusion, respiratory activity, and ATP synthesis, although weak coupling efficiency and reduced membrane potential was described for some patient cells (Loiseau *et al*., 2007; Amiott *et al*., 2008). In another study, the effect of CMT2A alleles on mitochondrial fusion was examined by expressing mutant Mfn2 proteins in double mitofusin knockout ($MFN1^{-/-}$ $MFN2^{-/-}$) MEFs (Detmer and Chan, 2007a). A subset of MEFs expressing mutant Mfn2 proteins had fusion-deficient mitochondria, others had normal fusion activity but aggregated mitochondria, and another subset had normal mitochondrial dynamics and distribution. Surprisingly, homozygous knockin of Mfn2 R94Q (a loss of fusion allele) yielded MEFs with no significant mitochondrial phenotypes (Detmer and Chan, 2007a), but transgenic mice overexpressing the Mfn2 T105M allele specifically in motor nerves had muscle atrophy and mobility defects that resemble CMT2A patient phenotypes (Detmer *et al*., 2008). Finally, overexpression of mutant Mfn2 proteins in cultured rat dorsal root ganglion (DRG) cells dominantly interfered with mitochondrial motility, causing accumulation of mitochondria in the cell body and impaired movement of mitochondria up and down axons (Baloh *et al*., 2007). Although informative, none of these studies have been able to clearly identify the molecular defect(s) responsible for axonal degeneration and CMT2A disease progression.

Because budding yeast express only one mitofusin gene, *FZO1*, the yeast protein may execute many of the shared and distinct activities performed by Mfn1 and Mfn2 in mammalian cells. The functional consequences of *MFN2* alleles can be readily studied in yeast because experiments are performed in cells expressing a single copy of the mutant gene. This eliminates the possibility of functional complementation by other mitofusin isoforms and allows easy detection of mutant-specific changes in protein expression, stability, localization, and modification. In addition, yeast do not require respiration for survival, so compensatory changes in metabolism that could occur in knockout MEFs or cultured patient cells expressing nonfunctional mitofusin proteins are avoided. Moreover, yeast mitochondria undergo directed, poleward movement from mother to daughter cell during budding (mitochondrial inheritance). Thus, defects in yeast mitochondrial inheritance may be observed if CMT2A alleles alter organelle motility. Based on these traits, the yeast model system has the potential to uncover disease-related defects in mitofusin function(s) that have been difficult or impossible to detect in CMT2A patient fibroblasts, mouse models, or mammalian cell culture systems.

In this study, we analyzed the in vitro GTPase activity and in vivo function of Fzo1 proteins harboring mutations analogous to CMT2A *MFN2* mutations. Our results reveal distinct phenotypic profiles for individual CMT2A alleles and show that not all substitutions have the predicted effect on the function of the domains in which they reside. In addition, we found that one mutation in the GTPase domain not only disrupts GTP hydrolysis and membrane fusion, but also leads to changes in ubiquitylation and stability of the mutant protein. These data support a novel connection between the Fzo1 GTPase cycle and the regulation of Fzo1 ubiquitylation and turnover that may be key to the regulation of mitochondrial dynamics.

MATERIALS AND METHODS

Yeast Strains and Growth Conditions

Strains used in this study (Supplemental Table S1) were constructed in the W303 genetic background unless otherwise indicated. Standard methods were used for growth, transformation, and genetic manipulation of *Saccharomyces cerevisiae* and *Escherichia coli* (Guthrie and Fink, 2001; Sambrook and Russell, 2001). The *FZO1* gene was cloned into single-copy *CEN* plasmids under control of the endogenous promoter and mutations were introduced using QuikChange site-directed mutagenesis (Stratagene, La Jolla, CA). All mutations were confirmed by DNA sequencing. Expression and localization

of wild type (WT) and mutant proteins were verified by Western blotting and subcellular fractionation.

Serial Dilution Analysis of Respiratory Growth

For serial dilutions, *fzo1*Δ or *FZO1* strains expressing the indicated plasmids were grown to log phase (OD_{600} = 0.7–1.5) at 30°C in selective synthetic medium containing 2% dextrose (SDM). Cells were pelleted and resuspended in 1 M sorbitol to a cell density of 0.5 OD_{600}. Serial 1:10 dilutions were spotted onto selective SDM and SGly (2% glycerol) plates and grown at 25, 30, or 37°C for 2 and 4 d, respectively.

Microscopic Analysis of Mitochondrial Morphology

Mitochondrial morphology was scored in WT and mutant cells expressing matrix-targeted green fluorescent protein (mito-GFP) (B1078; Supplemental Table S2). Strains were grown in selective SDM and scored in mid-log phase (OD_{600} = 0.7–1.0). Morphology phenotypes were assessed in at least 100 cells in three or more independent experiments. Data reported are the average and SD of all experiments. Cells were visualized on an Axioplan 2 imaging microscope (Carl Zeiss, Jena, Germany) with a 100× oil immersion objective. Digital fluorescence and differential interference contrast (DIC) images of cells were acquired using an AxioCam MRm monochrome digital camera. Z-stacks of 0.25-μm slices were obtained and deconvolved by Axiovision software (version 4.6; Carl Zeiss). Three-dimensional projections of mitochondria were generated with the Transparency (voxel) setting and converted to a single image. Final images were processed and assembled using Photoshop and Illustrator CS3 (Adobe Systems, Mountain View, CA).

In Vivo Mitochondrial Fusion Assay

Mitochondrial fusion in zygotes was examined essentially as described previously (Mozdy *et al*., 2000). Mitochondria in each haploid *fzo1*Δ *dnm1*Δ parent (expressing WT or mutant Fzo1 protein) were labeled with mito-GFP or mito-red fluorescent protein (RFP). Large-budded zygotes were scored for mitochondrial fusion 3–4 h after mating. Mitochondrial fusion was quantified in 50–100 zygotes per strain in three separate experiments. Data reported are the average and SD of all experiments.

Protein Extraction and Western Blotting

Whole cell extracts were prepared from 2.5 OD log-phase cells by using an alkaline extraction protocol (Kushnirov, 2000). An equal volume of supernatant (10 μl = 0.5 OD cells) was loaded on 8% SDS polyacrylamide gels and separated proteins were transferred to nitrocellulose membrane (Bio-Rad Laboratories, Hercules, CA) for Western blot analysis. Proteins were analyzed by Western blotting with antibodies specific for Fzo1 (1:2000) (Shaw laboratory), hemagglutinin (HA) (1:2500) (University of Utah Core Facility, Salt Lake City, UT), c-Myc clone 9E10 (1:5000) (Santa Cruz Biotechnology, Santa Cruz, CA), 3-phosphoglycerate kinase (3PGK) (1:10,000) (Invitrogen, Carlsbad, CA), or Mgm1 (1:3000) (a gift from A. Reichert, Ludwig-Maximilians-Universität München, München, Germany) and the appropriate horseradish peroxidase-conjugated secondary antibody. Immunodecorated proteins were detected using ECL Plus (GE Healthcare, Chalfont St. Giles, Buckinghamshire, United Kingdom) followed by exposure to film. Films were scanned by densitometry and bands were quantified using Quantity One software (Bio-Rad Laboratories). Alternatively, fluorescent secondary antibodies (IRDye 800 anti-mouse or IRDye 680 anti-rabbit; Li-Cor Biosciences, Lincoln, NE) were used and immunodecorated proteins were detected and quantified using an Odyssey scanner and Odyssey 3.0 analysis software (Li-Cor Biosciences).

Mitochondrial Isolation

Mitochondria were isolated from strains expressing HA and Myc-tagged WT or mutant Fzo1 protein as described previously (Meeusen *et al*., 2004), except that spheroplasting was carried out for 1 h at 30°C with 600 μl of Zymolyase 100T (US Biological, Swampscott, MA) per liter of culture and 1 mM phenylmethylsulfonyl fluoride was added to the mitochondrial resuspension buffer.

Fzo1–Fzo1 Coimmunoprecipitation (coIP)

Coimmunoprecipitation of HA and Myc tagged WT and mutant Fzo1 proteins was performed as described previously (Griffin and Chan, 2006). In brief, 50 OD cells were disrupted by glass bead lysis in 500 μl of lysis buffer (50 mM Tris-Cl, pH 7.4, 150 mM NaCl, 0.5 mM EDTA, 0.2% Triton X-100, and 1:500 Calbiochem Protease Inhibitor Cocktail Set III [Calbiochem, San Diego, CA]). Lysates were cleared by centrifugation and 400 μl of lysate was incubated with 40 μl (50% slurry) of anti-c-Myc agarose beads (A7470; Sigma-Aldrich, St. Louis, MO) at 4°C for 2 h. Beads were washed three times with lysis buffer and incubated in 50 μl of sample buffer (200 mM Tris-Cl, pH 6.8, 2% SDS, 20% glycerol, and 10 μg/ml bromphenol blue) at 65°C for 8 min before elution of bound proteins by centrifugation (1 min at 12,000 rpm). Samples (15 μl) were separated by 8% SDS-polyacrylamide gel electrophoresis (PAGE) and analyzed by Western blotting.

Fzo1 GTP Hydrolysis Assay

Mitochondria were isolated from *fzo1*Δ and *mdm30*Δ strains expressing HA and/or Myc-tagged Fzo1 proteins as described above. For each sample, 200 μg of mitochondrial protein was incubated in 300 μl of buffer A (20 mM PIPES-KOH, pH 6.8, 150 mM KOAc, 1.2 M sorbitol, and 5 mM EGTA) for 5 min on ice. Mitochondria were collected by centrifugation at 10,000 × *g* for 5 min at 4°C and washed in 300 μl of buffer A lacking EGTA. Mitochondrial pellets were suspended in 20 μl of buffer B (20 mM PIPES-KOH, pH 6.8, 150 mM KOAc, and 5 mM $Mg(OAc)_2$, 1.2 M sorbitol, and 0.5 mM GTP) and solubilized in 400 μl of IP buffer (1.5% Triton X-100, 150 mM NaCl, 30 mM HEPES-KOH, pH 7.4, and 0.5% Calbiochem Protease Inhibitor Cocktail Set III) for 10 min at 4°C with gentle agitation. After centrifugation at 12,500 × *g* for 10 min, supernatant was added to 40 μl (50% slurry) of anti-HA agarose conjugate (A2095; Sigma-Aldrich) or anti-c-Myc agarose conjugate (A7470; Sigma-Aldrich) in a Handee Spin Cup column (Pierce Chemical, Rockford, IL). Samples were incubated for two h at 4°C with gentle agitation followed by three washes with 400 μl of IP buffer. Bound Fzo1 protein was incubated in 100 μl of GTPase buffer (20 mM PIPES-KOH, pH 6.8, 150 mM KOAc, 5 mM $Mg(OAc)_2$, 0.5% Calbiochem Protease Inhibitor Cocktail Set III, 1 mM GTP, and 16.5 μM [α-^{32}P]GTP) at 30°C for 45 min. Products of the hydrolysis reaction were eluted from the bound protein by centrifugation (1 min at 5000 × *g*), and 5 μl of eluate was spotted on a Baker-Flex cellulose PEI-F thin layer chromatography (TLC) plate. [α-^{32}P]GTP and [α-^{32}P]GDP pools were separated by TLC using formic acid:LiCl solvent as described previously (Melen *et al*., 1994; Warnock *et al*., 1996; Fukushima *et al*., 2001), visualized on a Storm 820 PhosphorImager (GE Healthcare), and spots were quantified using Quantity One (Bio-Rad Laboratories) or ImageQuant (GE Healthcare) software. After elution of the GTPase reaction, bound protein was washed again (3 times with 400 μl of IP buffer). Fifty microliters of sample buffer was added to the beads, and bound protein was eluted by centrifugation after incubation at 65°C for 8 min. After boiling, samples (15 μl) were separated by 8% SDS-PAGE and analyzed by Western blotting to confirm IP and/or coIP of Fzo1 protein(s) and to rule out coIP of the inner membrane fusion GTPase Mgm1.

Fzo1–Mdm30 Coimmunoprecipitation

Spheroplasts were generated from 60 ODs of cells grown to mid-log phase and treated with 75 U of Zymolyase for 45 min at 30°C as described previously (Ingerman *et al*., 2007). Spheroplasts were resuspended in 1 ml of IP buffer (50 mM Tris-Cl, pH 7.5, 150 mM NaCl, 0.6% Triton X-100, 10% glycerol, and Complete mini protease inhibitor [Roche Diagnostics, Indianapolis, IN]) and incubated at 4°C for 30 min. Lysates were cleared by centrifugation at 13,000 rpm for 30 min, and supernatants were incubated with anti-HA Affinity Matrix (Roche Diagnostics) for 1 h at 4°C. Beads were washed with IP buffer and immunoprecipitated protein was eluted by heating in sample buffer before resolution by SDS-PAGE and analysis by anti-HA and anti-Myc Western blotting.

Fzo1 Protein Degradation Assays

Pulse-chase metabolic labeling was performed as described previously (Moreau *et al*., 1997; Cohen *et al*., 2008). In brief, cells were collected during exponential growth and incubated for 50 min at 23°C in 1 ml medium lacking methionine (SD-Met). Cells were pulsed with 25 Ci of [^{35}S]methionine (PerkinElmer Life and Analytical Sciences, Boston, MA) per OD of cells for 15 min at 30°C followed by 15 min at 37°C. After addition of 1 ml of chase medium (SD-Met supplemented with 6 mg/ml methionine and 2 mg/ml bovine serum albumin), cells were incubated at 37°C and 2 ODs of cells were collected immediately (time 0) and at 30 and 60 min after the chase. Samples were treated as described previously (Moreau *et al*., 1997), and results were quantified by Storm PhosphorImager and ImageQuant software (GE Healthcare). Error bars represent the SD from three independent experiments. Cycloheximide experiments were performed as described by Cohen *et al*. (2008).

Fzo1 Ubiquitylation Assay

Yeast extracts were prepared from 5 ODs of exponentially growing cells using the NaOH-trichloroacetic acid lysis method (Avaro *et al*., 2002). Extracts were incubated for 15 min at 70°C in SDS loading buffer and insoluble material removed by centrifugation for 5 min at 13,000 rpm. Supernatants were diluted 10-fold in IP buffer (50 mM Tris-Cl, pH 7.5, 500 mM NaCl, 0.6% Triton X-100, 10% glycerol, 20 mM iodoacetamide, and Complete mini protease inhibitor [Roche Diagnostics]) and incubated with EZ View anti-HA Affinity Matrix (Sigma-Aldrich) overnight at 4°C. Beads were washed with IP buffer and immunoprecipitated protein was eluted by heating in sample buffer before resolution by 6% SDS-PAGE and anti-HA Western blotting (12CA5 epitope; Weissman laboratory).

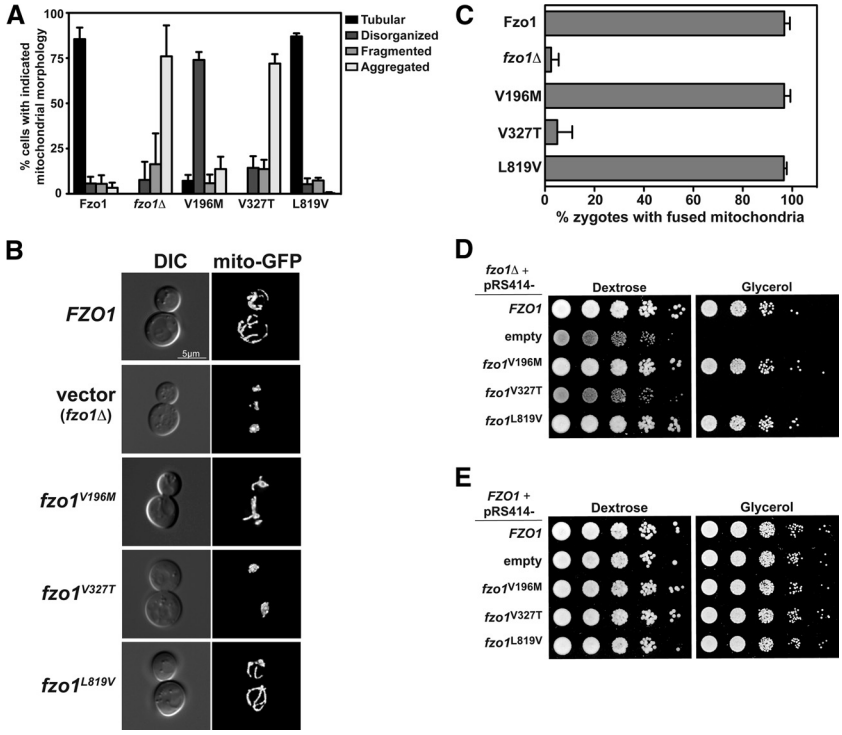

Figure 2. In vivo mitochondrial phenotypes of cells expressing mutant Fzo1 proteins. (A) Quantification of mitochondrial morphologies observed in cells expressing WT and mutant Fzo1 proteins. Bars and error bars represent the average and SD of at least three independent experiments. Samples are labeled according to the amino acid substitution in the protein being expressed. (B) Representative images of mitochondrial morphology in *fzo1*Δ cells expressing the indicated *FZO1* gene from the pRS414 plasmid. Mitochondria were visualized by expression of mito-GFP. (C) Quantification of mitochondrial fusion in *fzo1*Δ *dnm1*Δ cells expressing WT or mutant Fzo1 protein. The percentage of large-budded zygotes containing fused mitochondria (overlapping red and green mitochondrial tubules) in each strain is indicated. Bars and error bars represent the average and SD from three independent experiments. At least 50 zygotes were scored per experiment. (D and E) Dilution analysis of respiratory growth phenotypes in *fzo1*Δ (D) or *FZO1* (E) cells expressing the WT or mutant *FZO1* gene from the pRS414 plasmid. Each spot is a serial 1:10 dilution of cells grown on SD-TRP (dextrose) or SGly-TRP (glycerol) plates at 30°C.

RESULTS

CMT2A Alleles in Yeast Fzo1 Cause Mitochondrial Morphology, Fusion, or Respiration Phenotypes

The sequence homology between yeast Fzo1 and human Mfn2 is not extensive, but many CMT2A alleles are located within regions of Mfn2 that are conserved throughout the mitofusin family (Zuchner *et al*., 2004, 2006; Kijima *et al*., 2005; Lawson *et al*., 2005; Cartoni and Martinou, 2009). Based on conserved spacing relative to the canonical G1 and G3 functional motifs within the GTPase domain (Figure 1), we introduced Mfn2 T105M and I213T, two previously studied CMT2A alleles (Lawson *et al*., 2005; Amiott *et al*., 2008), into the yeast Fzo1 protein. V196M and V327T are the analogous mutations in the GTPase domain of Fzo1. Another CMT2A allele, Mfn2 L734V (Amiott *et al*., 2008), is predicted to lie in the "*d*" position of the C-terminal HR2 coiled-coil of Mfn2 (based on the COILS prediction program; Lupas *et al*., 1991). Mitofusin HR2 domains are proposed to mediate *trans*-mitofusin interactions that tether opposing mitochondrial membranes as an essential step in the fusion process (Koshiba *et al*., 2004). The analogous residue in Fzo1 (L819) has previously been mutated to proline (L819P) and was found to disrupt in vivo Fzo1 function (Griffin and Chan, 2006). We studied the effects of an L→V substitution at this conserved residue in Fzo1 (L819V), which mimics the Mfn2 L734V CMT2A allele (Figure 1).

The plasmid shuffle method was used to generate *fzo1*Δ yeast strains expressing WT or mutant *FZO1* and matrix-targeted green fluorescent protein (mito-GFP). These strains were used to determine the effect of mutant Fzo1 proteins on mitochondrial morphology. Although cells expressing WT and the L819V mutant displayed typical well-distributed and branched tubular mitochondrial networks, the V196M and V327T mutant strains exhibited abnormal mitochondrial morphology phenotypes (Figures 2, A and B). Mitochondria in the V196M mutant strain had an unusual intermediate morphology described here as "disorganized tubules" (Figure 2A). Mitochondria in these cells were tubular, but distorted, less branched, and poorly distributed throughout the cell (Figure 2B and Supplemental Figure S1). By transmission electron microscopy (TEM), mitochondria in the V196M strain were tubular organelles with normal inner membrane cristae (data not shown). The V327T strain contained tightly aggregated mitochondria, similar to those seen in cells lacking *FZO1* (vector or *fzo1*Δ cells) (Figure 2, A and B). TEM confirmed that the aggregates in the *fzo1*Δ and V327T cells were clusters of individual mitochondrial fragments rather than single swollen mitochondria (data not shown).

In other strain backgrounds, *fzo1*Δ cells have dispersed mitochondrial fragments instead of the aggregates we observed in W303 strain background. When we examined mitochondrial morphology in the FY strain background, aggregated mitochondrial fragments were observed in only 17% of the *fzo1*Δ cells. By contrast, 64% of the V327T mutant cells still had aggregated mitochondria in the FY background. This result suggests that both mitochondrial fragmentation and aggregation are phenotypes associated with the V327T mutation.

Importantly, all strains, including those with altered mitochondrial morphology, exhibited normal mitochondrial inheritance. Therefore, cells lacking *FZO1* (*fzo1*Δ), or expressing CMT2A mutant proteins that produce disorganized tubules (V196M), or mitochondrial aggregates (V327T), maintain faithful transfer of the organelle to the emerging bud.

Mitochondrial fragmentation can result from either a block in mitochondrial fusion or enhanced mitochondrial division. To determine whether the mutant Fzo1 proteins were able to mediate fusion, we performed an in vivo fusion assay. Cells expressing either mito-GFP or mito-RFP were mated and successful outer and inner membrane fusion was observed as overlapping fluorescent mitochondria in the zygote. This assay was performed in cells lacking one com-

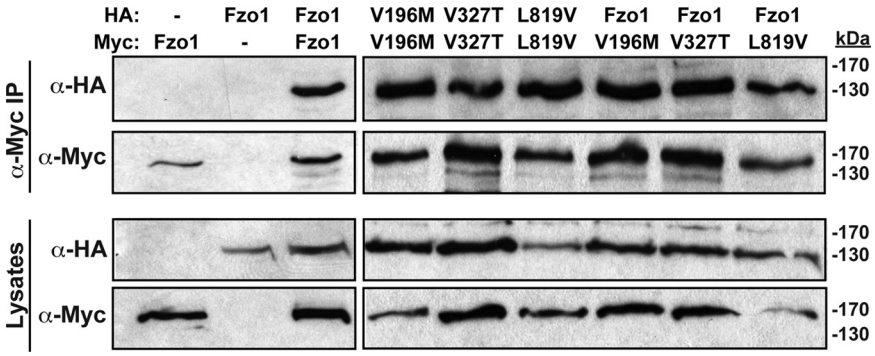

Figure 3. Coimmunoprecipitation of HA and Myc-tagged Fzo1 proteins. Lysates from cells expressing the indicated HA and Myc-tagged Fzo1 proteins were incubated with anti-Myc agarose beads. Lysates (bottom) and immunoprecipitated proteins (top) were resolved by SDS-PAGE and probed by Western blotting with anti-HA and anti-Myc antibodies.

ponent of both the fission and fusion machineries (*fzo1*Δ *dnm1*Δ) to maintain mitochondrial tubules and prevent the loss of mtDNA and membrane potential that occurs upon fragmentation (Hermann *et al*., 1998; Rapaport *et al*., 1998; Mozdy *et al*., 2000). When the mutant Fzo1 proteins were introduced into the *fzo1*Δ *dnm1*Δ strain and mated, all but the *fzo1*Δ and V327T mutant strains showed significant mitochondrial fusion in large-budded zygotes (Figure 2C). These results suggest that the V327T mutation renders the protein nonfunctional for fusion and are consistent with the dramatic change in mitochondrial morphology described above. These data also suggest that the altered morphology observed in the V196M strain is not related to the ability of the mutant protein to function as a fusion molecule. When each mutant protein was expressed in WT cells, mitochondria in all strains formed tubular networks and were able to fuse as well as those in a WT strain (data not shown). Thus, the V196M and V327T mutants do not have dominant-negative effects on mitochondrial morphology or fusion.

The effect of mutant proteins on mitochondrial respiratory function was determined by growing strains on the nonfermentable carbon source, glycerol. Consistent with the morphology and fusion phenotypes described above, *fzo1*Δ cells expressing no Fzo1 protein (empty) or the V327T mutant protein were not able to grow on glycerol at 25, 30, or 37°C (Figure 2D). The other mutant strains (V196M and L819V) grew as well as WT on both dextrose and glycerol medium at all temperatures. The ability to grow on glycerol was normal in cells expressing mutant Fzo1 proteins in a WT strain background (Figure 2E). These data confirm that none of the tested mutants cause dominant-negative defects and indicate that a functional Fzo1 protein can suppress morphology, respiration, and fusion defects caused by these CMT2A alleles.

CMT2A Mutations Do Not Affect Fzo1–Fzo1 Complex Formation

Fzo1 exists in high molecular weight complexes in vivo (Rapaport *et al*., 1998). Fzo1–Fzo1 interactions are required for fusion and presumably occur in *trans* (on adjacent mitochondrial membranes) as well as in *cis* (within the same membrane)(Meeusen *et al*., 2004). CoIP experiments have shown that Fzo1 proteins form homotypic oligomers (Griffin and Chan, 2006), similar to the homo and heterotypic complexes reported for Mfn1 and Mfn2 (Chen *et al*., 2003). An anchored C-terminal HR1/HR2 domain efficiently recruits the N-terminal HR0/GTPase domain to mitochondria, suggesting that Fzo1–Fzo1 interactions occur between the C-terminal and N-terminal portions of the protein (Griffin and Chan, 2006). However, interactions may also occur between the same domain of different molecules, because proteins with the S201N mutation in the GTPase domain display reduced self-association (Griffin and Chan, 2006).

To determine whether CMT2A point mutations in the GTPase and HR2 domains interfere with Fzo1-Fzo1 complex formation, we performed coIP experiments by using HA and Myc-tagged WT and CMT2A mutant Fzo1 proteins. When coexpressed, each of the mutant Fzo1 proteins was able to coIP both itself and the WT protein equally well (Figure 3). These data indicate that V196M, V327T, and L819V point mutations have no gross effect on Fzo1–Fzo1 complex formation, even though the L819 residue is predicted to be involved in HR2 coiled-coil formation. Combined with the observation that cells coexpressing WT and mutant proteins lack in vivo phenotypes, our results indicate that these CMT2A mutant proteins form functional complexes with the WT protein and do not have dominant negative effects on WT protein function.

Fzo1 Is an Authentic GTPase and the V327T Mutant Protein Is Defective for GTP Hydrolysis

The GTPase domain of Fzo1 is highly conserved and mammalian mitofusins have been shown to harbor GTPase activity (Ishihara *et al*., 2004). However, GTP hydrolysis by Fzo1 has never been demonstrated. We evaluated Fzo1 GTP hydrolysis by incubating [α^{32}P]GTP with immunoprecipitated WT and mutant Fzo1 proteins (Figure 4A). Products of the hydrolysis reaction were separated and analyzed by TLC. Proof of concept for this experiment was established using Myc-tagged Fzo1 and three GTPase domain mutants: K200A, S201N, and T221A (Figure 4B). These residues are conserved in the G1 and G2 motifs of the Fzo1 GTPase domain and based upon similar mutations in Ras proteins, are predicted to be essential for GTP binding and hydrolysis (Figure 1). After a 45-min incubation with immunoprecipitated WT Fzo1, a substantial portion of input [α^{32}P]GTP was converted to [α^{32}P]GDP (Figure 4B, lane 2). However, none of the immunoprecipitated GTPase mutant proteins hydrolyzed GTP (Figure 4B, lanes 3–5). These data establish that Fzo1 is a bona fide GTPase and that conserved motifs within the GTPase domain are essential for activity.

We analyzed CMT2A mutant Fzo1 proteins by using the same assay (Figure 4C). The V196M and L819V proteins efficiently hydrolyzed GTP, but the V327T protein had virtually no GTPase activity, comparable with the *fzo1*Δ sample (Figure 4C). This result indicates that the V327T substitution abolishes the enzymatic activity of the Fzo1 protein, consistent with the mitochondrial fragmentation, loss of fusion, and respiratory growth phenotypes of *fzo1*Δ cells expressing the V327T mutant protein (Figure 2). However, *FZO1* cells expressing the V327T mutant have no mitochondrial phenotypes, suggesting that WT–V327T Fzo1 complexes are func-

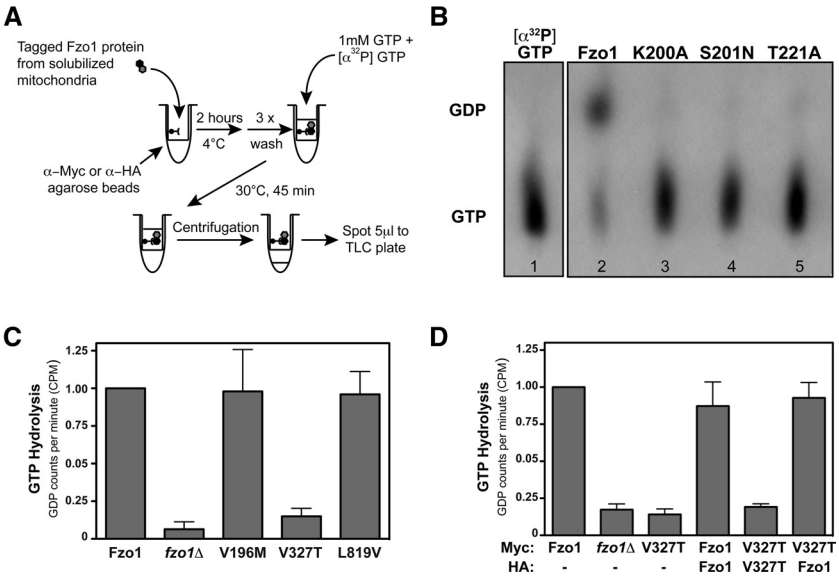

Figure 4. An assay for GTP hydrolysis by immunoprecipitated Fzo1 protein. (A) A schematic detailing the steps for immunoprecipitation of Fzo1 protein from isolated mitochondria and the subsequent analysis of GTP hydrolysis by the immobilized protein. (B) Example of TLC separation of radiolabeled GDP from nonhydrolyzed GTP. The initial buffer containing [α-^{32}P]GTP was spotted in the lane 1. The conversion of GTP to GDP by WT Fzo1 protein is shown in lane 2. Three Fzo1 proteins with GTPase domain mutations (K200A, S201N, and T221A) have no GTP hydrolysis activity (lanes 3, 4, and 5). (C) WT and mutant HA-tagged Fzo1 proteins were immunoprecipitated from isolated mitochondria and incubated with [α-^{32}P]GTP. The average amount of [α-^{32}P]GDP (a measure of GTP hydrolysis) generated by each mutant protein relative to WT is shown in the graph. Bars and error bars are the average and SD from three independent experiments. (D) Mitochondria isolated from strains expressing HA and Myc-tagged WT or V327T Fzo1 protein(s) were used to IP or coIP the indicated proteins. Fzo1 protein(s) immobilized on anti-Myc agarose beads were incubated with [α-^{32}P]GTP and the amount of [α-^{32}P]GDP generated by GTP hydrolysis was measured relative to WT. Bars and error bars are the average and SD from three independent experiments.

tional for GTP hydrolysis. To test this, HA-Fzo1 was coimmunoprecipitated by Myc-V327T (ensuring that WT protein would be present in the GTPase reaction only if associated with the mutant protein) and incubated with [α^{32}P]GTP. As predicted, WT–V327T complexes were able to efficiently hydrolyze GTP (Figure 4D). Although the average amount of [α^{32}P] GDP generated in WT-V327T reactions was comparable with WT–WT reactions, this assay is not controlled for potential differences in the amount of mutant or WT protein immunoprecipitated. Therefore, our analysis provides a qualitative, rather than a quantitative, measure of enzyme activity by WT and mutant protein complexes. In total, these experiments demonstrate that Fzo1 is a GTPase and that V327T disrupts GTPase activity but that complexes containing both WT and V327T Fzo1 proteins are functional for GTP hydrolysis. As a consequence, mitochondrial membrane fusion and function are normal in cells expressing both forms of the protein.

The V327T Mutation Alters Ubiquitylation and Turnover of the Fzo1 Protein

During the evaluation of mitochondrial phenotypes associated with CMT2A alleles, the expression and mitochondrial localization of the mutant proteins was confirmed by anti-Fzo1 Western blotting of whole cell extracts and mitochondrial fractions (Figure 5A; data not shown). Unexpectedly, we consistently observed that the relative abundance of the V327T mutant protein was slightly but reproducibly greater than that of WT and the other mutant proteins (Figure 5A). Fzo1 protein levels are regulated, at least in part, by the F-box protein Mdm30 (Fritz *et al*., 2003; Neutzner and Youle, 2005; Durr *et al*., 2006; Escobar-Henriques *et al*., 2006). Turnover of Fzo1 protein occurs via ubiquitin-dependent proteasomal degradation (Cohen *et al*., 2008), and Mdm30 represents the substrate recognition component of the SCF^{Mdm30} ubiquitin ligase. Because Fzo1 was shown previously to interact with Mdm30 (Escobar-Henriques *et al*., 2006), we examined the interaction between the V327T mutant and SCF^{Mdm30}. Although both HA-Fzo1 and HA-V327T proteins coIP Mdm30-Myc, the relative ratios of protein suggest a decrease in Mdm30 association with HA-V327T (Figure 5B). Based on this observation, we compared the rate of degradation of WT and V327T Fzo1 proteins. Both pulse-chase metabolic labeling (Figure 5C) and cycloheximide chase (data not shown) revealed a decreased rate of degradation of the V327T mutant protein relative to WT Fzo1, similar to the stabilization of WT Fzo1 observed in *mdm30*Δ strains (Fritz *et al*., 2003; Neutzner and Youle, 2005; Durr *et al*., 2006; Escobar-Henriques *et al*., 2006; Cohen *et al*., 2008).

To determine whether the observed reduction in V327T mutant protein degradation results from changes in ubiquitylation, we immunoprecipitated HA-tagged WT and mutant proteins and probed for ubiquitylated HA-Fzo1 species by Western blotting (Figure 5D). As reported previously (Cohen *et al*., 2008), long exposures revealed at least two ubiquitin-conjugated species of HA-Fzo1 migrating just above the 150-kDa marker (Figure 5D, lane 2). Immunodetection of the HA-V327T mutant (Figure 5D, lane3) showed that the proportion of ubiquitin-conjugated species is noticeably reduced, even though there is more HA-V327T protein present in the sample (Figure 5D, bottom). These data indicate that ubiquitylation of the V327T mutant protein is compromised, perhaps as a result of reduced interactions between Fzo1 and SCF^{Mdm30} (Figure 5B).

Fzo1 Stability and Ubiquitylation Are Linked to GTP Hydrolysis

Significantly, V327T was the only CMT2A mutant protein that was stabilized, and it was also the only mutant protein that had lost the ability to hydrolyze GTP, suggesting a possible link between these two events. To investigate whether loss of GTPase activity causes Fzo1 protein stabilization, we compared steady-state levels of Fzo1 in *mdm30*Δ cells to steady-state levels of GTPase domain mutant Fzo1 proteins that are either "GTPase-active" or "GTPase-dead" (Figure 6A). Consistent with a loss of Fzo1 ubiquitylation (*mdm30*Δ), each of the GTPase-dead mutants (K200A, S201N, and V327T) was ~1.5-fold more abundant than WT, whereas the GTPase-active mutant (V196M) was present at WT levels. We also determined Fzo1 protein levels in cells

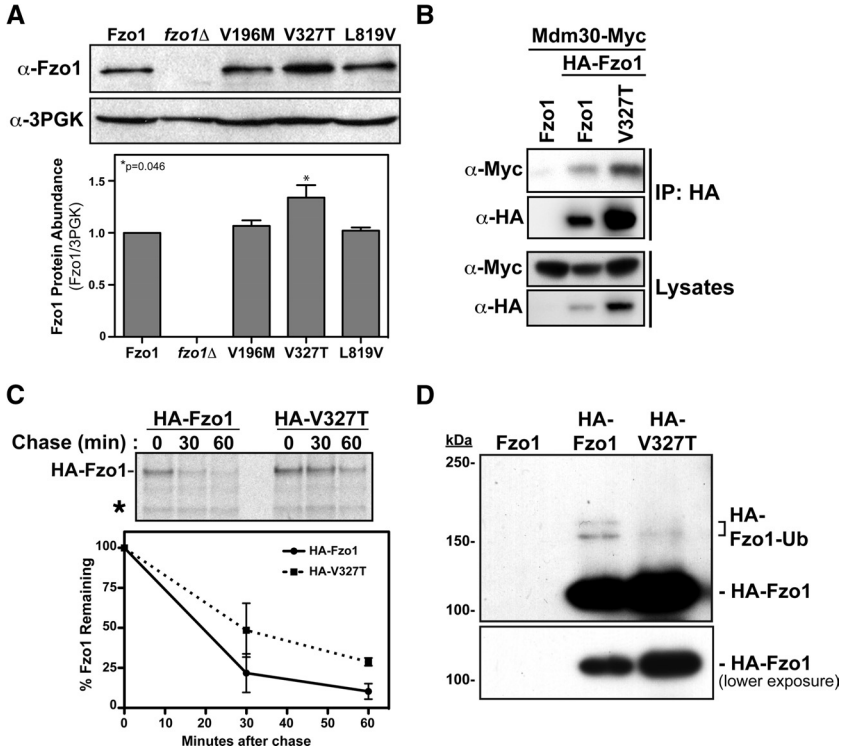

Figure 5. Stabilization and delayed turnover of the V327T mutant protein is associated with diminished Mdm30 interaction and reduced ubiquitylation. (A) Steady-state abundance of WT and mutant proteins expressed in *fzo1*Δ cells. Whole cell extracts were immunoblotted with anti-Fzo1 and anti-3PGK antibodies. The density of each Fzo1 protein band was normalized to 3PGK signal in the same sample. The average abundance of Fzo1 protein in each strain is plotted relative to the WT sample. Error bars indicate the SEM from several blots. The asterisk indicates statistical significance ($p < 0.05$) by *t* test (GraphPad Prism Software, La Jolla, CA). (B) Mdm30-Myc was coimmunoprecipitated from cell lysates (bottom) by HA-Fzo1 and HA-V327T (top). The amount of Mdm30-Myc coimmunoprecipitated relative to HA-Fzo1 protein is reduced in the HA-V327T strain. (C) HA-Fzo1 protein turnover was analyzed by ^{35}S pulse-chase metabolic labeling in WT and V327T mutant strains. Samples were collected and analyzed at 0, 30, and 60 min after the chase was initiated. The asterisk indicates a nonspecific band. The percentage of ^{35}S-Fzo1 protein remaining at each time point is plotted. Data points are the average and error bars are the SD from three independent experiments. (D) HA-Fzo1and HA-V327T proteins were immunoprecipitated from cell lysates and probed with anti-HA antibody to detect ubiquitylated forms of the tagged Fzo1 protein (HA-Fzo1-Ub, top). A lower exposure of the same blot (bottom) shows the levels of nonubiquitylated HA-Fzo1 species.

defective for mitochondrial fission (*dnm1*Δ) or fusion (*mgm1*Δ and *ugo1*Δ). Fzo1 levels were unchanged in the absence of fission (*dnm1*Δ), whereas the loss of either Mgm1 or Ugo1 had the opposite effect, reducing Fzo1 protein to approximately half the normal steady-state level (Figure 6A). These results demonstrate that the observed stabilization of Fzo1 in the GTPase mutants is not an indirect effect caused by loss of mitochondrial dynamics.

Because WT-V327T complexes are able to hydrolyze GTP (Figure 4D), we postulated that the V327T mutant protein would no longer be stabilized in cells coexpressing WT and V327T Fzo1 proteins. Analysis of extracts from cells express-

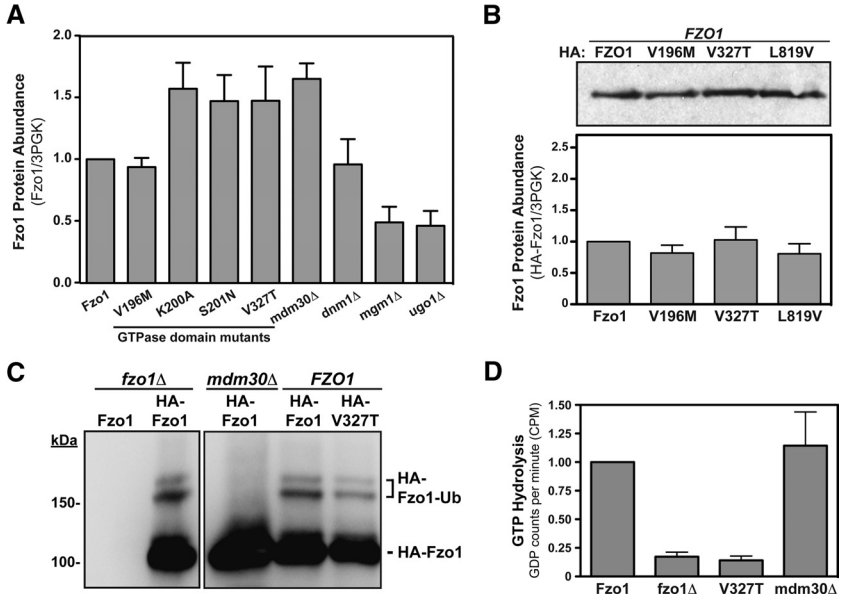

Figure 6. Turnover and ubiquitylation of HA-V327T is restored in the presence of WT Fzo1 protein and GTPase activity does not require Mdm30. (A) Steady-state abundance of WT and mutant Fzo1 proteins in whole cell extracts from the indicated yeast strains. Protein bands were detected using a fluorescent secondary antibody followed by scanning on an Odyssey imaging system (Li-Cor Biosciences). The average intensity of each Fzo1 protein band was normalized to 3PGK signal. Bars represent the abundance of Fzo1 protein in each strain relative to the WT sample. Error bars indicate the SEM from at least three blots. (B) Steady-state abundance of HA-tagged WT and mutant proteins expressed in *FZO1* cells. Whole cell extracts were immunoblotted with anti-HA and anti-3PGK antibodies. The average intensity of each HA band was normalized to 3PGK signal. Bars represent the abundance of HA-Fzo1 protein in each strain relative to the WT sample. Error bars indicate the SEM from at least three blots. (C) HA-Fzo1and HA-V327T proteins were immunoprecipitated from cell lysates and probed with anti-HA antibody to detect ubiquitylated forms of the tagged Fzo1 protein. HA-Fzo1 in *mdm30*Δ cells is not ubiquitylated. HA-V327T is ubiquitylated in cells that also express WT Fzo1. (D) HA-tagged Fzo1 protein was immunoprecipitated from the indicated isolated mitochondria and incubated with [α-^{32}P]GTP. Bars represent the mean [α-^{32}P]GDP generated by Fzo1 protein from each strain relative to WT. Error bars are the SD from three independent experiments.

ing only HA-tagged Fzo1 proteins shows that steady-state levels of HA-V327T are greater than HA-Fzo1 and the other mutant proteins (Supplemental Figure S2). By contrast, in cells coexpressing untagged Fzo1 and HA-tagged WT or mutant proteins, the level of HA-V327T protein is equivalent to WT (Figure 6B). The presence of ubiquitylated HA-V327T species in cells coexpressing WT and mutant Fzo1 (Figure 6C) confirms that a return to normal steady-state protein levels correlates with restoration of ubiquitylation. Thus, ubiquitylation and turnover of the mutant protein is normal when WT Fzo1 and HA-V327T proteins form a GTPase-active complex. As shown in Figure 6D, we also find that HA-Fzo1 is an active GTPase in *mdm30*Δ cells. This result suggests that neither Mdm30, nor Fzo1 ubiquitylation are required to trigger the GTPase activity of Fzo1. Instead, our data indicate that Fzo1-Mdm30 associations and subsequent ubiquitylation and turnover of Fzo1 are closely linked to, or perhaps regulated by, the Fzo1 GTPase cycle.

DISCUSSION

Using the single yeast mitofusin Fzo1 as a model, we performed phenotypic analysis of Mfn2 mutations linked to CMT2A neuropathy. Our experiments provide new evidence that yeast Fzo1 is a bona fide GTPase and identify a key residue, downstream of the G3 motif (Fzo1 V327), which is essential for GTP hydrolysis. Importantly, the V327T substitution also reduces ubiquitylation and association with the F-box protein Mdm30, resulting in stabilization of the mutant protein. Other CMT2A mutations had different and less dramatic effects on Fzo1 function, resulting in either no phenotype, or a subtle perturbation of mitochondrial morphology. Thus, we find that CMT2A mutations have variable effects on Fzo1 function, including defects in mitochondrial morphology, fusion, GTP hydrolysis, and ubiquitylation. In addition, although CMT2A is a dominantly inherited disease, CMT2A mutations in Fzo1 are not dominant negative for function.

Based on the conserved functional domains of mitofusin proteins, it has been presumed that CMT2A mutations in the GTPase domain would disrupt GTP hydrolysis, and substitutions in HR2 would perturb coiled-coil formation and mitochondrial tethering. Although we and others have shown that mitochondrial membrane fusion is blocked by mutations that disrupt GTPase activity (Hermann *et al*., 1998; Santel *et al*., 2003; Ishihara *et al*., 2004; Meeusen *et al*., 2004; this study), the current study demonstrates that the V196M GTPase mutant protein fully supports GTP hydrolysis and fusion. Similarly, the L819V mutation in the HR2 domain has no detrimental effects on Fzo1–Fzo1 complex formation or fusion. Our results indicate that CMT2A mutations may not exclusively affect Mfn2-mediated mitochondrial fusion, or the predicted function of the domains in which they reside.

The V196M mutant Fzo1 protein can self-interact by coIP, is an active GTPase, and is competent for fusion. The only noticeable V196M phenotype is a nondominant change in mitochondrial morphology that does not affect respiratory growth. Thus, even though this mutation is in the GTPase domain and positioned just a few residues upstream of the conserved G1 motif, the mutant protein is functional. By contrast, the analogous Mfn2 T105M mutant protein is nonfunctional for fusion and has weak interactions with WT Mfn1 and Mfn2 (Detmer and Chan, 2007a). The molecular basis for differences between the yeast and mammalian mutant proteins is unclear. In the future, it will be essential to determine whether the T105M Mfn2 protein hydrolyzes GTP. If the T105M mutant protein is GTPase active, then T105 may be important for other protein–protein interactions or posttranslational modifications that occur in mammalian cells. For example, the region just upstream of T105 (Mfn2 residues 77–91) is implicated in associations between Mfn2 and Ras that are proposed to affect ERK signaling (Chen *et al*., 2004; McBride *et al*., 2006; Pawlikowska *et al*., 2007; de Brito and Scorrano, 2009). Alternatively, if Mfn2 T105M is GTPase defective, the T105 residue may make a critical contribution to the fold or function of the Mfn2 GTPase domain that is not required in Fzo1.

In yeast, mitochondrial inheritance is a measure of mitochondrial motility. Expression of CMT2A Mfn2 alleles in DRG axons inhibits mitochondrial motility, suggesting there is a connection between Mfn2 function and axonal transport of mitochondria (Baloh *et al*., 2007). We looked for differences in mitochondrial distribution between mother and daughter cells in the CMT2A mutant Fzo1 strains. Although deletion of Fzo1 (*fzo1*Δ) and expression of mutant proteins caused changes in morphology, which might be expected to alter motility, mitochondrial inheritance was unaffected. It is not clear whether the absence of an inheritance defect in yeast indicates that mitofusins do not play a direct role in organelle motility, or whether it is simply a consequence of different requirements for mitochondrial movement in yeast and mammalian cells. In yeast, mitochondria move along actin filaments (Fehrenbacher *et al*., 2004) via myosin motor proteins (Itoh *et al*., 2002, 2004; Altmann *et al*., 2008), whereas mammalian mitochondria primarily move along microtubules via kinesin and dynein motors (Hollenbeck and Saxton, 2005; Pilling *et al*., 2006).

We found that the V327T mutation has a dramatic effect on Fzo1 function. Not only is the mutant protein unable to restore respiratory growth and fusion activity in an *fzo1*Δ strain, the mutation abrogates GTP hydrolysis, and partially blocks Fzo1 interaction with Mdm30, ubiquitylation, and degradation. Ubiquitin-mediated degradation of Mfn2 has not been demonstrated but cannot be ruled out, because a mitochondrial E3 ubiquitin ligase called MARCH V has been reported to interact with Mfn2 (Nakamura *et al*., 2006). Other RING-finger ubiquitin ligases have also recently been identified as important in maintaining mitochondrial homeostasis (Yonashiro *et al*., 2006; Karbowski *et al*., 2007; Neutzner *et al*., 2008).

Our data provide evidence for a novel relationship between Fzo1 GTP hydrolysis, ubiquitylation, degradation, and membrane fusion. Specifically, we have shown that loss of GTP hydrolysis impairs ubiquitylation and degradation of Fzo1, whereas hydrolysis is unaffected by the absence of ubiquitylation (*mdm30*Δ cells). These findings place the GTPase activity of Fzo1 upstream of Mdm30-mediated ubiquitylation and degradation in the fusion pathway. We propose that Fzo1 ubiquitylation and turnover are controlled by the GTPase cycle and suggest that ubiquitylation may be a regulated and important step in Mfn2 function that should be considered when evaluating CMT2A alleles. Consistent with overexpression experiments, the possibility that some alleles may stabilize the mutant Mfn2 protein by interfering with ubiquitylation and turnover suggests that changes in the ratio of WT to mutant mitofusin proteins could be sufficient to promote the disease state.

CMT2A is an autosomal dominant genetic disease, yet even the most severe Fzo1 disease allele, V327T, is functionally recessive in the presence of WT Fzo1. Similarly, WT mitofusin (Mfn1) complements nonfunctional Mfn2 alleles in MEFs, and CMT2A alleles must be overexpressed in cultured neurons or mouse models to produce mitochon-

drial or neurological phenotypes, respectively. In mice, loss of either mitofusin (Mfn1 or Mfn2) is embryonic lethal, whereas CMT2A patients experience very specific and progressive degeneration of axons in the peripheral nerves rather than systemic pathology. These observations suggest that although functional defects caused by some CMT2A mutations can be striking in isolation, they are likely to be more subtle in their native environment, perhaps even undetectable in nonneuronal cell types or by assays currently being used in the clinic and laboratory. Because age at onset and penetrance vary considerably within and between CMT2A patient families, it is also possible that environmental factors or other complex genetic traits or polymorphisms influence disease severity and progression.

ACKNOWLEDGMENTS

We thank Huyen Bui for preliminary work with the L819V mutant, Jane Macfarlane for expertise in mutagenesis and plasmid construction, Adam Day for technical assistance, and J. Michael McCaffery at the Integrated Imaging Center of Johns Hopkins University for TEM analysis. E.A.A. is currently supported by a research grant from the United Mitochondrial Disease Foundation (UMDF 08-064 Mitochondrial Fusion Defects in Neurological Disease) and previously received support from the National Institutes of Health T32 institutional training grant 5 T32 HD07576-22. Additional research support was provided by the Charcot-Marie-Tooth Association (Y.S.-G.), the Intramural Research Program of the National Institutes of Health, National Cancer Institute, Center for Cancer Research (to A.M.W.), and National Institutes of Health grant GM-53466 (to J.M.S.). Support for sequencing, antibody, and oligonucleotide services at the University of Utah is provided by a National Center for Research Resources grant (M01-RR00064; to L. Betz, P.I.).

REFERENCES

Altmann, K., Frank, M., Neumann, D., Jakobs, S., and Westermann, B. (2008). The class V myosin motor protein, Myo2, plays a major role in mitochondrial motility in *Saccharomyces cerevisiae*. J. Cell Biol. *181*, 119–130.

Amiott, E. A., Lott, P., Soto, J., Kang, P. B., McCaffery, J. M., DiMauro, S., Abel, E. D., Flanigan, K. M., Lawson, V. H., and Shaw, J. M. (2008). Mitochondrial fusion and function in Charcot-Marie-Tooth type 2A patient fibroblasts with mitofusin 2 mutations. Exp. Neurol. *211*, 115–127.

Avaro, S., Belgareh-Touze, N., Sibella-Arguelles, C., Volland, C., and Haguenauer-Tsapis, R. (2002). Mutants defective in secretory/vacuolar pathways in the EUROFAN collection of yeast disruptants. Yeast *19*, 351–371.

Baloh, R. H. (2008). Mitochondrial dynamics and peripheral neuropathy. Neuroscientist *14*, 12–18.

Baloh, R. H., Schmidt, R. E., Pestronk, A., and Milbrandt, J. (2007). Altered axonal mitochondrial transport in the pathogenesis of Charcot-Marie-Tooth disease from mitofusin 2 mutations. J. Neurosci. *27*, 422–430.

Brooks, C., Wei, Q., Feng, L., Dong, G., Tao, Y., Mei, L., Xie, Z. J., and Dong, Z. (2007). Bak regulates mitochondrial morphology and pathology during apoptosis by interacting with mitofusins. Proc. Natl. Acad. Sci. USA *104*, 11649–11654.

Cartoni, R., and Martinou, J. C. (2009). Role of Mitofusin 2 mutations in the physiopathology of Charcot-Marie-Tooth disease type 2A. Exp. Neurol. *218*, 268–273.

Chen, H., and Chan, D. C. (2006). Critical dependence of neurons on mitochondrial dynamics. Curr. Opin. Cell Biol. *18*, 453–459.

Chen, H., Chomyn, A., and Chan, D. C. (2005). Disruption of fusion results in mitochondrial heterogeneity and dysfunction. J. Biol. Chem. *280*, 26185–26192.

Chen, H., Detmer, S. A., Ewald, A. J., Griffin, E. E., Fraser, S. E., and Chan, D. C. (2003). Mitofusins Mfn1 and Mfn2 coordinately regulate mitochondrial fusion and are essential for embryonic development. J. Cell Biol. *160*, 189–200.

Chen, K. H., Guo, X., Ma, D., Guo, Y., Li, Q., Yang, D., Li, P., Qiu, X., Wen, S., Xiao, R. P., and Tang, J. (2004). Dysregulation of HSG triggers vascular proliferative disorders. Nat. Cell Biol. *6*, 872–883.

Chung, K. W., *et al*. (2006). Early onset severe and late-onset mild Charcot-Marie-Tooth disease with mitofusin 2 (MFN2) mutations. Brain *129*, 2103–2118.

Cipolat, S., Martins de Brito, O., Dal Zilio, B., and Scorrano, L. (2004). OPA1 requires mitofusin 1 to promote mitochondrial fusion. Proc. Natl. Acad. Sci. USA *101*, 15927–15932.

Cohen, M. M., Leboucher, G. P., Livnat-Levanon, N., Glickman, M. H., and Weissman, A. M. (2008). Ubiquitin-proteasome-dependent degradation of a mitofusin, a critical regulator of mitochondrial fusion. Mol. Biol. Cell *19*, 2457–2464.

de Brito, O. M., and Scorrano, L. (2008a). Mitofusin 2 tethers endoplasmic reticulum to mitochondria. Nature *456*, 605–610.

de Brito, O. M., and Scorrano, L. (2008b). Mitofusin 2, a mitochondria-shaping protein with signaling roles beyond fusion. Antioxid. Redox Signal. *10*, 621–633.

de Brito, O. M., and Scorrano, L. (2009). Mitofusin-2 regulates mitochondrial and endoplasmic reticulum morphology and tethering: the role of Ras. Mitochondrion *9*, 222–226.

Detmer, S. A., and Chan, D. C. (2007a). Complementation between mouse Mfn1 and Mfn2 protects mitochondrial fusion defects caused by CMT2A disease mutations. J Cell Biol. *176*, 405–414.

Detmer, S. A., and Chan, D. C. (2007b). Functions and dysfunctions of mitochondrial dynamics. Nat. Rev. *8*, 870–879.

Detmer, S. A., Vande Velde, C., Cleveland, D. W., and Chan, D. C. (2008). Hindlimb gait defects due to motor axon loss and reduced distal muscles in a transgenic mouse model of Charcot-Marie-Tooth type 2A. Hum. Mol. Genet *17*, 367–375.

Durr, M., Escobar-Henriques, M., Merz, S., Geimer, S., Langer, T., and Westermann, B. (2006). Nonredundant roles of mitochondria-associated F-box proteins Mfb1 and Mdm30 in maintenance of mitochondrial morphology in yeast. Mol. Biol. Cell *17*, 3745–3755.

Escobar-Henriques, M., Westermann, B., and Langer, T. (2006). Regulation of mitochondrial fusion by the F-box protein Mdm30 involves proteasome-independent turnover of Fzo1. J. Cell Biol. *173*, 645–650.

Eura, Y., Ishihara, N., Yokota, S., and Mihara, K. (2003). Two mitofusin proteins, mammalian homologues of FZO, with distinct functions are both required for mitochondrial fusion. J. Biochem. *134*, 333–344.

Fehrenbacher, K. L., Yang, H. C., Gay, A. C., Huckaba, T. M., and Pon, L. A. (2004). Live cell imaging of mitochondrial movement along actin cables in budding yeast. Curr. Biol. *14*, 1996–2004.

Fritz, S., Weinbach, N., and Westermann, B. (2003). Mdm30 is an F-box protein required for maintenance of fusion-competent mitochondria in yeast. Mol. Biol. Cell *14*, 2303–2313.

Fukushima, N. H., Brisch, E., Keegan, B. R., Bleazard, W., and Shaw, J. M. (2001). The GTPase effector domain sequence of the Dnm1p GTPase regulates self-assembly and controls a rate-limiting step in mitochondrial fission. Mol. Biol. Cell *12*, 2756–2766.

Griffin, E. E., and Chan, D. C. (2006). Domain interactions within Fzo1 oligomers are essential for mitochondrial fusion. J. Biol. Chem. *281*, 16599–16606.

Guthrie, C., and Fink, G. (2001). Methods in Enzymology: Guide to Yeast Genetics and Molecular and Cellular Biology, New York: Academic Press.

Hales, K. G., and Fuller, M. T. (1997). Developmentally regulated mitochondrial fusion mediated by a conserved, novel, predicted GTPase. Cell *90*, 121–129.

Hermann, G. J., Thatcher, J. W., Mills, J. P., Hales, K. G., Fuller, M. T., Nunnari, J., and Shaw, J. M. (1998). Mitochondrial fusion in yeast requires the transmembrane GTPase Fzo1p. J Cell Biol. *143*, 359–373.

Hollenbeck, P. J. (2005). Mitochondria and neurotransmission: evacuating the synapse. Neuron *47*, 331–333.

Hollenbeck, P. J., and Saxton, W. M. (2005). The axonal transport of mitochondria. J Cell Sci. *118*, 5411–5419.

Ingerman, E., Meeusen, S., Devay, R., and Nunnari, J. (2007). In vitro assays for mitochondrial fusion and division. Methods Cell Biol. *80*, 707–720.

Ishihara, N., Eura, Y., and Mihara, K. (2004). Mitofusin 1 and 2 play distinct roles in mitochondrial fusion reactions via GTPase activity. J. Cell Sci. *117*, 6535–6546.

Itoh, T., Toh, E. A., and Matsui, Y. (2004). Mmr1p is a mitochondrial factor for Myo2p-dependent inheritance of mitochondria in the budding yeast. EMBO J. *23*, 2520–2530.

Itoh, T., Watabe, A., Toh, E. A., and Matsui, Y. (2002). Complex formation with Ypt11p, a rab-type small GTPase, is essential to facilitate the function of Myo2p, a class V myosin, in mitochondrial distribution in *Saccharomyces cerevisiae*. Mol. Cell. Biol. *22*, 7744–7757.

Karbowski, M., Lee, Y. J., Gaume, B., Jeong, S. Y., Frank, S., Nechushtan, A., Santel, A., Fuller, M., Smith, C. L., and Youle, R. J. (2002). Spatial and temporal association of Bax with mitochondrial fission sites, Drp1, and Mfn2 during apoptosis. J Cell Biol. *159*, 931–938.

Karbowski, M., Neutzner, A., and Youle, R. J. (2007). The mitochondrial E3 ubiquitin ligase MARCH5 is required for Drp1 dependent mitochondrial division. J Cell Biol. *178*, 71–84.

Kijima, K., *et al*. (2005). Mitochondrial GTPase mitofusin 2 mutation in Charcot-Marie-Tooth neuropathy type 2A. Hum. Genet. *116*, 23–27.

Koshiba, T., Detmer, S. A., Kaiser, J. T., Chen, H., McCaffery, J. M., and Chan, D. C. (2004). Structural basis of mitochondrial tethering by mitofusin complexes. Science *305*, 858–862.

Kushnirov, V. V. (2000). Rapid and reliable protein extraction from yeast. Yeast *16*, 857–860.

Lawson, V. H., Graham, B. V., and Flanigan, K. M. (2005). Clinical and electrophysiologic features of CMT2A with mutations in the mitofusin 2 gene. Neurology *65*, 197–204.

Loiseau, D., *et al*. (2007). Mitochondrial coupling defect in Charcot-Marie-Tooth type 2A disease. Ann. Neurol. *61*, 315–323.

Lupas, A., Van Dyke, M., and Stock, J. (1991). Predicting coiled coils from protein sequences. Science *252*, 1162–1164.

McBride, H. M., Neuspiel, M., and Wasiak, S. (2006). Mitochondria: more than just a powerhouse. Curr. Biol. *16*, R551–R560.

Meeusen, S., McCaffery, J. M., and Nunnari, J. (2004). Mitochondrial fusion intermediates revealed in vitro. Science *305*, 1747–1752.

Meeusen, S. L., and Nunnari, J. (2007). Mitochondrial fusion in vitro. Methods Mol. Biol. *372*, 461–466.

Melen, K., Ronni, T., Lotta, T., and Julkunen, I. (1994). Enzymatic characterization of interferon-induced antiviral GTPases murine Mx1 and human MxA proteins. J. Biol. Chem. *269*, 2009–2015.

Moreau, V., Galan, J. M., Devilliers, G., Haguenauer-Tsapis, R., and Winsor, B. (1997). The yeast actin-related protein Arp2p is required for the internalization step of endocytosis. Mol. Biol. Cell *8*, 1361–1375.

Mozdy, A. D., McCaffery, J. M., and Shaw, J. M. (2000). Dnm1p GTPase-mediated mitochondrial fission is a multi-step process requiring the novel integral membrane component Fis1p. J. Cell Biol. *151*, 367–380.

Nakada, K., Inoue, K., Ono, T., Isobe, K., Ogura, A., Goto, Y. I., Nonaka, I., and Hayashi, J. I. (2001). Inter-mitochondrial complementation: mitochondria-specific system preventing mice from expression of disease phenotypes by mutant mtDNA. Nat. Med. *7*, 934–940.

Nakamura, N., Kimura, Y., Tokuda, M., Honda, S., and Hirose, S. (2006). MARCH-V is a novel mitofusin 2- and Drp1-binding protein able to change mitochondrial morphology. EMBO Rep. *7*, 1019–1022.

Neutzner, A., Benard, G., Youle, R. J., and Karbowski, M. (2008). Role of the ubiquitin conjugation system in the maintenance of mitochondrial homeostasis. Ann. N.Y. Acad. Sci. *1147*, 242–253.

Neutzner, A., and Youle, R. J. (2005). Instability of the mitofusin Fzo1 regulates mitochondrial morphology during the mating response of the yeast *Saccharomyces cerevisiae*. J. Biol. Chem. *280*, 18598–18603.

Nunnari, J., Marshall, W. F., Straight, A., Murray, A., Sedat, J. W., and Walter, P. (1997). Mitochondrial transmission during mating in *Saccharomyces cerevisiae* is determined by mitochondrial fusion and fission and the intramitochondrial segregation of mitochondrial DNA. Mol. Biol. Cell *8*, 1233–1242.

Okamoto, K., and Shaw, J. M. (2005). Mitochondrial morphology and dynamics in yeast and multicellular eukaryotes. Annu. Rev. Genet. *39*, 503–536.

Ono, T., Isobe, K., Nakada, K., and Hayashi, J. I. (2001). Human cells are protected from mitochondrial dysfunction by complementation of DNA products in fused mitochondria. Nat. Genet. *28*, 272–275.

Pawlikowska, P., Gajkowska, B., and Orzechowski, A. (2007). Mitofusin 2 (Mfn2): a key player in insulin-dependent myogenesis in vitro. Cell Tissue Res. *327*, 571–581.

Pilling, A. D., Horiuchi, D., Lively, C. M., and Saxton, W. M. (2006). Kinesin-1 and Dynein are the primary motors for fast transport of mitochondria in *Drosophila* motor axons. Mol. Biol. Cell *17*, 2057–2068.

Rapaport, D., Brunner, M., Neupert, W., and Westermann, B. (1998). Fzo1p is a mitochondrial outer membrane protein essential for the biogenesis of functional mitochondria in *Saccharomyces cerevisiae*. J. Biol. Chem. *273*, 20150–20155.

Rojo, M., Legros, F., Chateau, D., and Lombes, A. (2002). Membrane topology and mitochondrial targeting of mitofusins, ubiquitous mammalian homologs of the transmembrane GTPase Fzo. J. Cell Sci. *115*, 1663–1674.

Sambrook, J., and Russell, D. (2001). Molecular Cloning: A Laboratory Manual, 3rd ed., Cold Spring Harbor, MA: Cold Spring Harbor Laboratory Press.

Santel, A., Frank, S., Gaume, B., Herrler, M., Youle, R. J., and Fuller, M. T. (2003). Mitofusin-1 protein is a generally expressed mediator of mitochondrial fusion in mammalian cells. J. Cell Sci. *116*, 2763–2774.

Santel, A., and Fuller, M. T. (2001). Control of mitochondrial morphology by a human mitofusin. J. Cell Sci. *114*, 867–874.

Sesaki, H., and Jensen, R. E. (1999). Division versus fusion: Dnm1p and Fzo1p antagonistically regulate mitochondrial shape. J Cell Biol. *147*, 699–706.

Skre, H. (1974). Genetic and clinical aspects of Charcot-Marie-Tooth's disease. Clin. Genet. *6*, 98–118.

Verhoeven, K., *et al*. (2006). MFN2 mutation distribution and genotype/phenotype correlation in Charcot-Marie-Tooth type 2. Brain *129*, 2093–2102.

Verstreken, P., Ly, C. V., Venken, K. J., Koh, T. W., Zhou, Y., and Bellen, H. J. (2005). Synaptic mitochondria are critical for mobilization of reserve pool vesicles at Drosophila neuromuscular junctions. Neuron *47*, 365–378.

Warnock, D. E., Hinshaw, J. E., and Schmid, S. L. (1996). Dynamin self-assembly stimulates its GTPase activity. J. Biol. Chem. *271*, 22310–22314.

Yonashiro, R., *et al*. (2006). A novel mitochondrial ubiquitin ligase plays a critical role in mitochondrial dynamics. EMBO J. *25*, 3618–3626.

Zuchner, S., *et al*. (2006). Axonal neuropathy with optic atrophy is caused by mutations in mitofusin 2. Ann. Neurol. *59*, 276–281.

Zuchner, S., *et al*. (2004). Mutations in the mitochondrial GTPase mitofusin 2 cause Charcot-Marie-Tooth neuropathy type 2A. Nat. Genet. *36*, 449–451.